Making Sense of Incidental Musculoskeletal Findings on Breast MRI

Paul Wojack, MD; Suzanne McElligott, MD; Pamela Walsh, MD; Nina Vincoff, MD; Ekta Gupta, MD

Owing to its high sensitivity for cancer detection and superior soft-tissue resolution, MRI is often used for breast cancer staging and high-risk screening. Because it utilizes a dedicated coil with a large field of view, the modality often reveals incidental findings in extramammary structures of the chest wall and upper abdomen, particularly the musculature, ribs, and sternum.

To help radiologists gain confidence in interpretation and avoid unnecessary workups, we review the appearance of several of the most common musculoskeletal lesions demonstrated by breast MRI.

Figure 1. T1 fat-saturated, postcontrast axial MR image demonstrating T1 hypointense, nonenhancing mass in the sternum (circle). Additionally, this lesion was hypointense on all other sequences, consistent with a bone island.

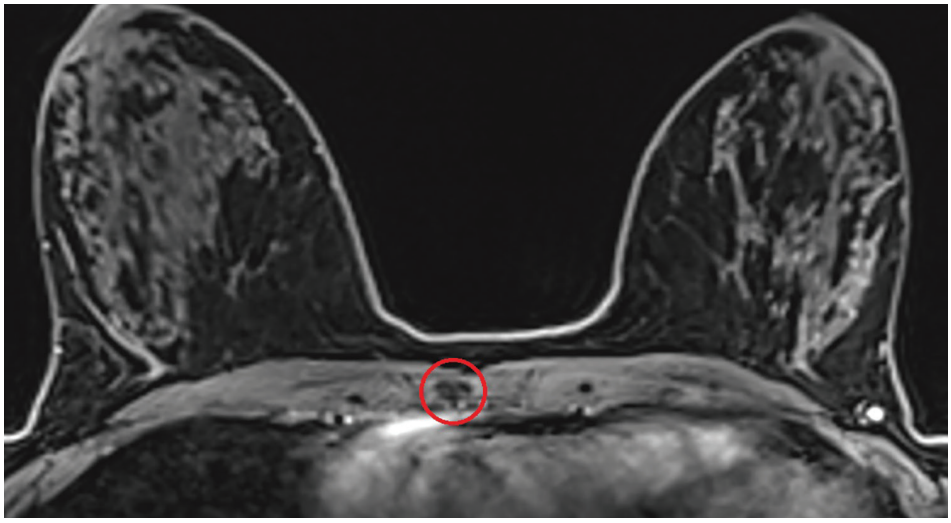

Frequency and Location of Incidental Findings

There is little question that breast MRI frequently makes incidental findings in the course of an examination performed for breast cancer screening or staging. In one study, extramammary findings were detected in up to 34% of patients.[1] While the liver and lungs are the most common sites for these entities, the chest musculature, ribs, and sternum are also common locations. Accounting for 7-10% of extramammary findings,[2,3,4] these incidental lesions may include osseous hemangiomas (also described as venous malformations), which comprise 17% of clinically insignificant abnormalities, and osseous metastases, which comprise 39% of clinically significant findings.[1]

Most lesions are determined to be benign, however up to 14% require additional workup.[1] Among patients with metastatic breast cancer, for example, about 60% will have osseous metastases.[5] Benign and malignant lesions, moreover, frequently share overlapping imaging features, making diagnosis challenging in many cases. Following is a discussion of the appearances of such entities that are likely to be encountered on breast MRI.

Benign Osseous Lesions

Bone Islands

Extremely common benign lesions, bone islands consist of masses of compacted cortical bone often seen in the sternum or ribs. Clinically asymptomatic, they do not enhance with contrast. While most occur sporadically, they can be associated with

Affiliations: Department of Radiology, Northwell Health, and Zucker School of Medicine at Hofstra/Northwell, Hempstead, New York. Disclosures: Dr. Vincoff is a member of the Editorial Advisory Board of *Applied Radiology.*
Keywords: extramammary breast MRI findings, benign and malignant osseous and soft tissue chest wall tumors, rib and sternal fractures, normal chest wall variants

Figure 2. (A) Axial T1 and (B) T2 fat-saturated MR images demonstrating a T1 isointense and T2 hyperintense mass in the sternum (circles). This mass demonstrated signal dropout on T1 fat-suppressed images and had mild enhancement (not shown). Findings are consistent with an osseous hemangioma.

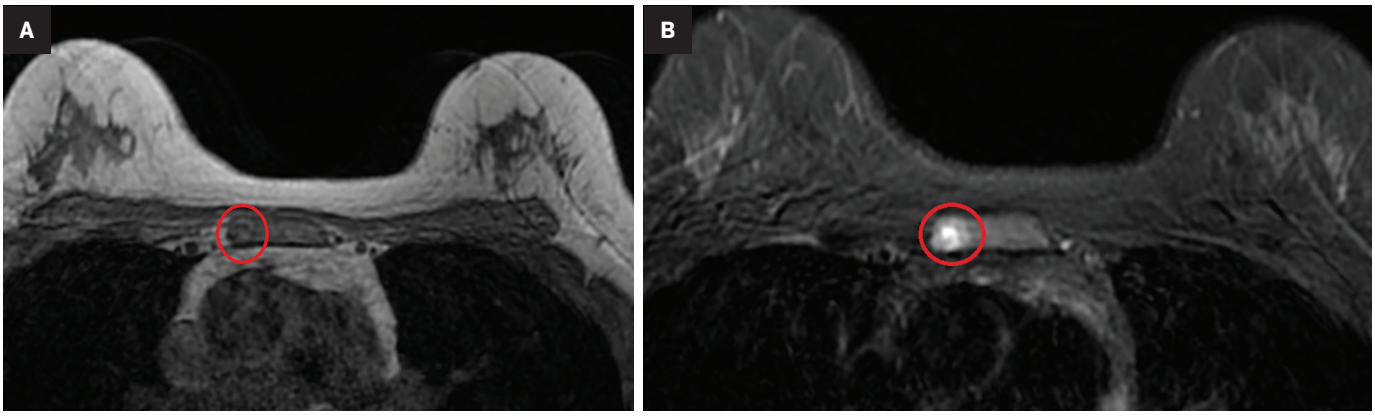

Figure 3. (A) Axial T2 fat-suppressed MR image showing a mass projecting anteriorly from the left third rib (red arrow). Note the T2 hyperintense cartilaginous cap of the lesion (white arrow). (B) Chest CT demonstrates corticomedullary continuity with the adjacent rib. Findings are consistent with an osteochondroma.

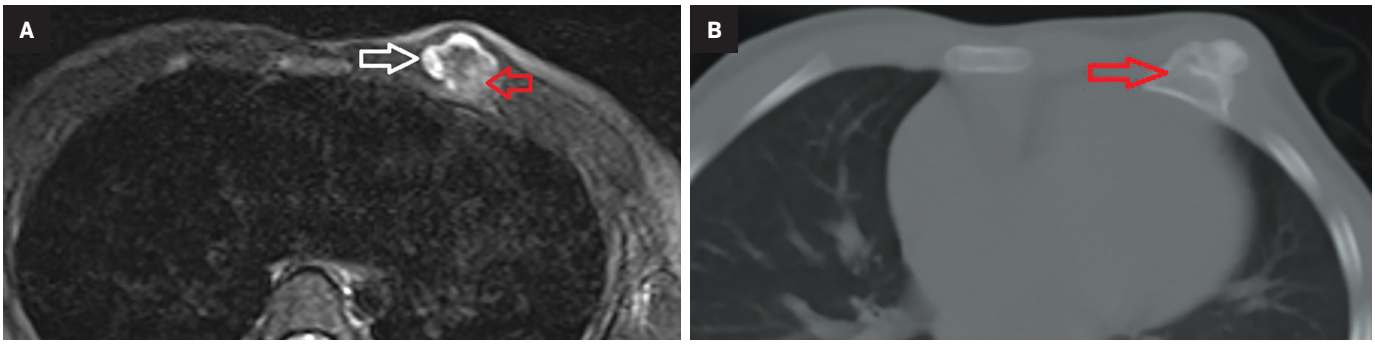

syndromes such as osteopoikilosis and Gardner syndrome (osteopoikilosis plus colonic polyps). Appearing highly sclerotic with a mean attenuation of 885 HU or greater on CT, they are deeply hypointense on all sequences on breast MRI (Figure 1).[6,7]

Hemangiomas

Osseous hemangiomas are often seen within the sternum (Figure 2). Histologically, they are composed of vascular elements with associated fat, although other components such as smooth muscle, fibrous tissue, or bone may also be seen.[8,9] Most occur sporadically, but they can be associated with a wide variety of syndromes, in which case they more often affect the extremities.[9] They are T2 hyperintense with intermediate to high T1 signal (depending on the amount of fat within the lesion) and will typically enhance. Hemangiomas may be associated with radiating trabecular thickening around the lesion; however, this finding is better appreciated with CT or radiography. Unlike osseous hemangiomas elsewhere in the body, vertebral hemangiomas have characteristic vertically oriented trabeculations, which develop as a response to the axial loading forces.[9]

Osteochondromas

As a type of exostosis, osteochondromas consist of an osseous protrusion from a bone with an associated cartilage cap. They commonly occur in the long bones and sometimes within the ribs (Figure 3).[10] Solitary osteochondromas have a low (< 1%) chance of malignant degeneration to chondrosarcoma, although the risk is greater when they are associated with syndromes such as multiple hereditary exostoses (~5%).[11] On MRI, the osseous portion of the lesion demonstrates corticomedullary contiguity with adjacent bone. The cartilage cap has low-to-intermediate T1 and high T2 signal. A cartilage cap thickness >1.5 cm is suspicious for malignant degeneration.[11] Osteochondromas may present either asymptomatically or as palpable or painful masses if they impinge on adjacent neurovascular structures or muscles.

Fibrous Dysplasia

Fibrous dysplasia develops when immature bone and fibrous stroma replace normal cancellous bone as a result of abnormal differentiation of osteoblasts.[12] The condition commonly involves the ribs, skull, mandible, and long bones.[13] It can affect patients of all ages but is most common in children and young adults. Occurring sporadically, most cases are monostotic (involving

Figure 4. (A) Axial T2 fat-suppressed MR image showing a T2 hyperintense expansile lesion in the right fourth rib (arrow). This lesion had intermediate T1 signal and enhanced with contrast (not shown). (B) Subsequent axial CT image with contrast demonstrates ground-glass matrix within the lesion (arrow). No aggressive features were seen. Findings are compatible with fibrous dysplasia.

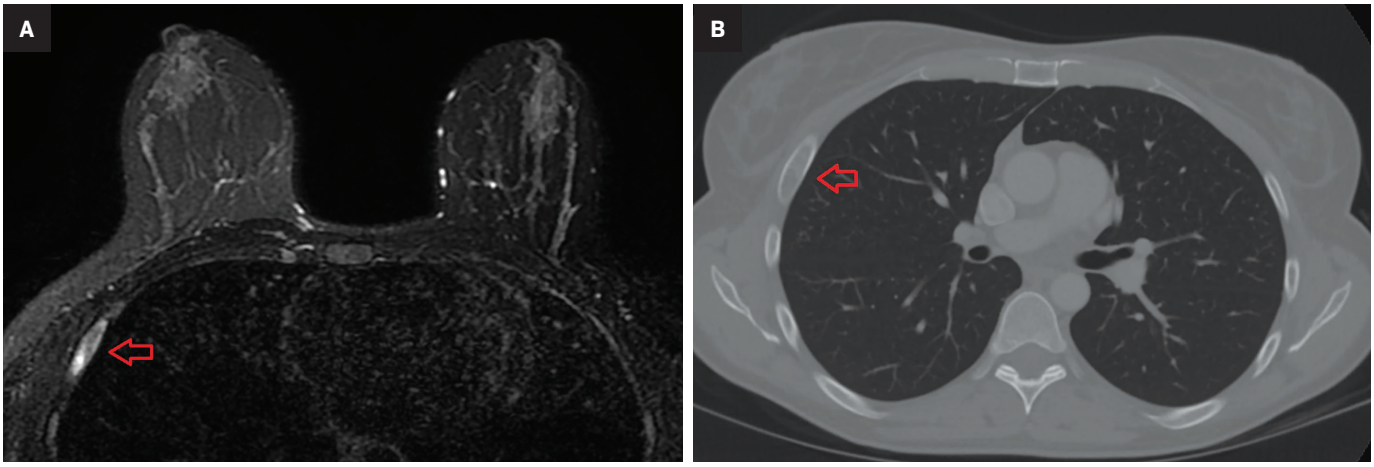

Figure 5. (A) Axial T1 and (B) T1 fat-suppressed postcontrast MR images of the right breast. There is a nonenhancing, T1 hyperintense mass in the lateral chest wall musculature that has signal loss on fat-suppressed sequence consistent with an intramuscular lipoma (circles).

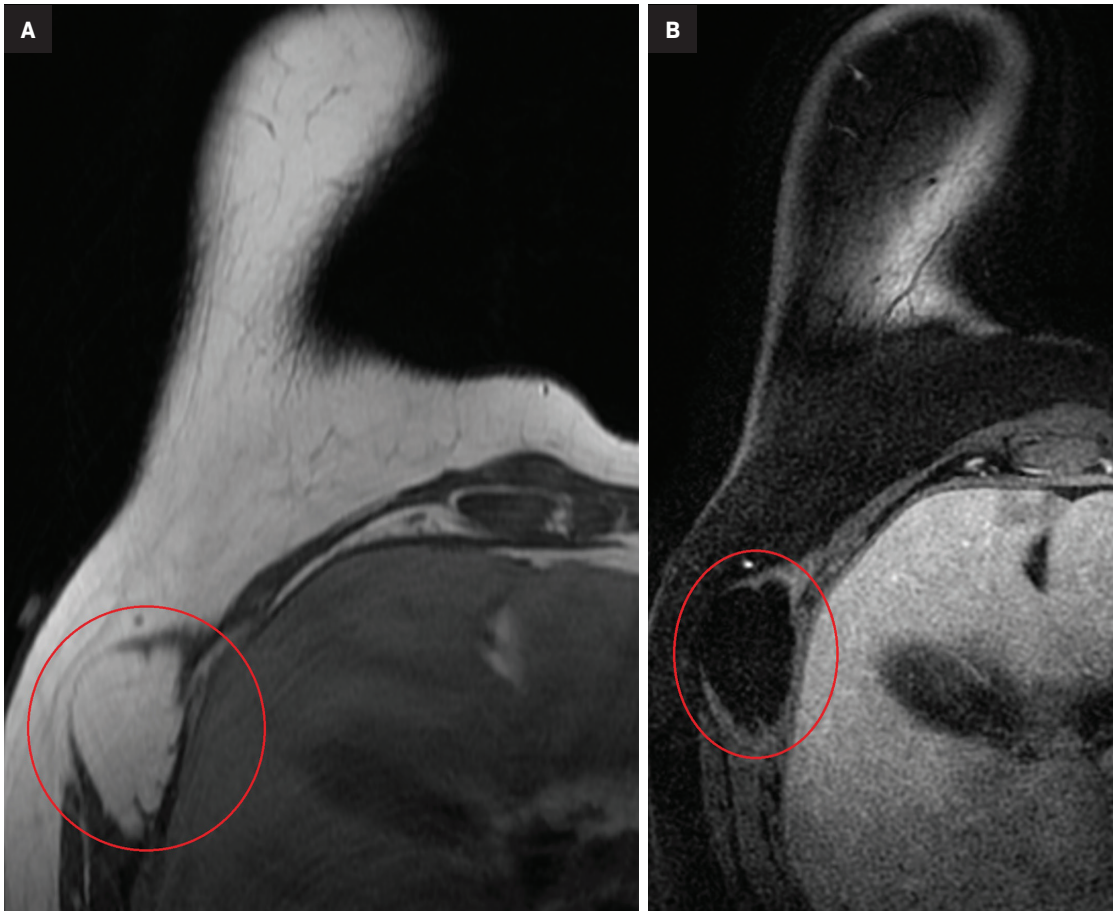

only one bone),[12] while about 20% are polyostotic (involving multiple bones) and may be associated with syndromes such as McCune-Albright and Mazabraud. Common MRI features consist of an expansile mass with low-to-intermediate T1 signal, variable T2 signal, and variable enhancement. If fibrous dysplasia is suspected, CT evaluation can help to demonstrate its typical "ground glass" matrix (Figure 4); diagnosis can often be made with imaging alone if this characteristic finding is present. Pathologic fractures are a potential complication. Malignant degeneration to osteosarcoma, fibrosarcoma, and malignant fibrous

Figure 6. (A) Axial STIR and (B) T2 fat-suppressed MR images demonstrating peripheral nerve sheath tumors in two separate patients. (A) A T2 hyperintense intercostal mass (circle) pathologically proven to represent an intercostal schwannoma. (B) Two T2 hyperintense, cutaneous masses in the lateral right breast and chest wall (arrows), consistent with neurofibromas in this patient with known type 1 neurofibromatosis. These masses demonstrated homogeneous enhancement in both patients (not shown), typical of peripheral nerve sheath tumors.

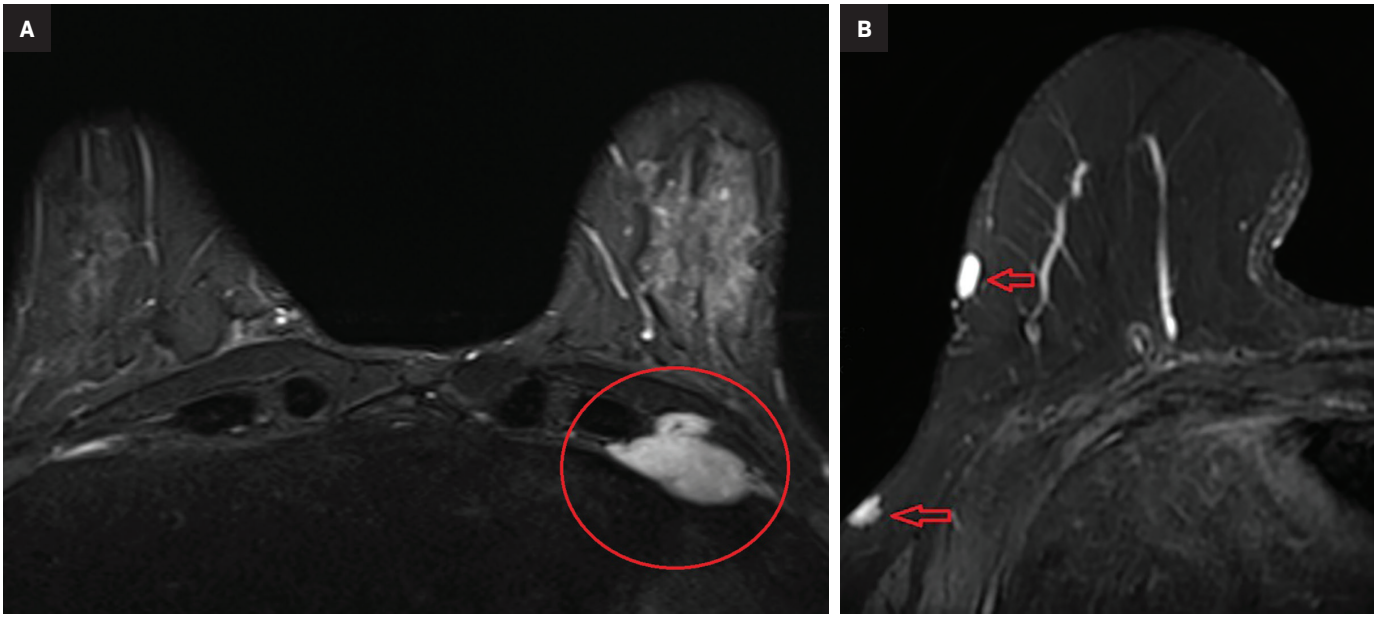

Figure 7. Axial T1 fat-suppressed precontrast MR image demonstrating a structure anterior to the medial aspect of the right pectoralis major musculature (arrow). This structure is isointense to skeletal muscle on all sequences and is compatible with a sternalis muscle.

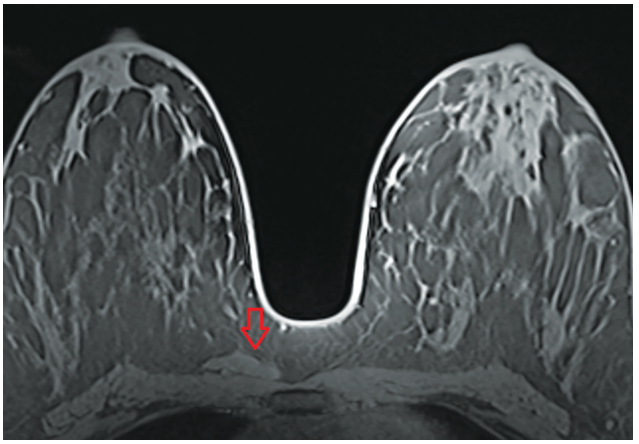

Figure 8. Axial T2 fat-suppressed MR image at the level of the sternoclavicular joints. There is a T2 hyperintense, well-circumscribed lesion adjacent to the left sternoclavicular joint (red arrow). This lesion was T1 hypointense and did not enhance, consistent with a cyst. Mild periarticular spurring is also seen at the left sternoclavicular joint (white arrow). Findings are consistent with osteoarthritis with subchondral cystic change.

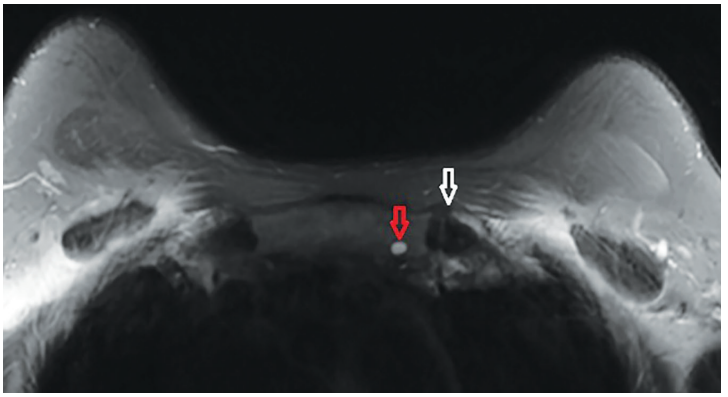

histiocytoma can also occur, albeit rarely (< 1% of cases).[12]

Benign Soft-tissue Masses

Lipoma

Composed of adipose tissue (Figure 5), these masses commonly present in the trunk and proximal extremities of middle-aged patients.[14] They appear as a circumscribed mass with signal characteristics of fat: high T1 and T2 signal with signal dropout on fat-suppressed sequences. Enhancement should be minimal or absent, although a few thin internal septa are normal. Any thick septations, nodularity, or prominent areas of enhancement should prompt further evaluation for a potential liposarcoma. When describing lipomas, their location is important to note, as superficial lipomas are easier to remove surgically than their intra- and intermuscular counterparts.

Nerve Sheath Tumors

Schwannomas and neurofibromas are common nerve sheath tumors that occur in the chest wall, typically in young and middle-aged adults.[15] They arise from the intercostal nerves or posteriorly from the spinal nerve roots. On MRI, they are isointense to slightly hyperintense

Figure 9. (A) Axial T2 fat-suppressed MR image showing a T2 hyperintense area in the sternum (circle). (B) Sagittal T1 postcontrast shows that this area represents a portion of the nonossified fibrocartilaginous disk of the normal manubriosternal joint.

relative to skeletal muscle on T1, hyperintense on T2, and enhance homogeneously with contrast.[16] Intercostal schwannomas are interposed between the ribs, reflecting the course of the intercostal nerves (Figure 6). Given their slow growth, there may be mild scalloping or remodeling of the adjacent bones.

Neurofibromas develop in younger patients, usually in their 20s and 30s, and are typically associated with type 1 neurofibromatosis.[15] They typically present as T2 hyperintense cutaneous masses (Figure 6). Some neurofibromas have a characteristic target-like appearance on T2 images; the periphery of the mass is brighter owing to the higher content of stromal material in the periphery relative to the cellular core.[17] This zonal distribution also results in more avid central enhancement of neurofibromas.

Other benign nerve sheath tumors such as ganglioneuromas and paragangliomas occur in the paraspinal regions and are less likely to be seen on breast MRI.

Sternalis Muscle

The sternalis muscle is an accessory muscle that runs vertically along the lateral margin of the sternum. Breast imagers are familiar with this anatomic variant, as it is seen on mammography and breast MRI. It typically originates from the upper sternum but demonstrates many potential insertions: the pectoral fascia, lower ribs, costal cartilages, rectus abdominis muscle sheath, and the aponeurosis of the abdominal external oblique muscle.[18,19] Mammographically, the muscle can present as an asymmetry in the posterior inner breast on the craniocaudal view. On MRI, it presents as a vertically oriented muscle just superficial to the medial aspect of the pectoralis major muscle, adjacent to the lateral margins of the sternum. It is isointense to the adjacent skeletal muscle on all sequences (Figure 7).

Sternal Arthridities

Multiple joints involving the sternum include the manubriosternal joint, the sternoclavicular joints, and multiple sternocostal joints. Like others, these joints are susceptible to various arthridities. The most common is osteoarthritis, which is characterized by joint space narrowing, periarticular osteophyte formation, and subchondral cystic changes. Subchondral cystic changes appear as T2 hyperintense cystic spaces within the bone and adjacent to the joint spaces (Figure 8).

Inflammatory arthridities can also be encountered. Rheumatoid arthritis may demonstrate periarticular erosions and joint-space narrowing, with fusion across the manubriosternal joint.[20] Psoriatic arthritis also presents with erosions but in a setting of superimposed osseous productive changes.[21] Although rare, crystalline arthropathies such as gout and calcium pyrophosphate dehydrate deposition disease (CPPD) can also affect the joints of the sternum.

A few other conditions classically involve the sternum. For example, SAPHO syndrome (synovitis, acne, psoriasis, hyperostosis, and osteitis) presents as sternocostoclavicular hyperostosis and osteitis on chest wall imaging.[22]

Monoarthritis of the manubriosternal joint, characterized by erosive changes about the joint, may also occur; this condition is often idiopathic but can occur in the setting of trauma or palmoplantar pustulosis.[23]

Tiezte syndrome is characterized by painful costochondritis of the costal cartilage.[23] It commonly occurs in young women. On imaging, the affected cartilage will appear enlarged with increased T2 signal in surrounding tissues and bone resulting from edema.

Additionally, the fibrocartilaginous disk of the manubriosternal joint demonstrates wide variability in resorption rate and degree as well as ossification over time. Therefore,

Figure 10. (A) Axial T2 fat-suppressed MR image demonstrates an acute left anterior rib fracture; the angulated, disrupted appearance of the rib cortex (arrow), along with a history of recent chest wall trauma, helped to confirm the diagnosis of acute fracture. Mild T2-hyperintense edema is seen surrounding the fracture site. (B) T1 postcontrast subtracted MR image through the sternum in a different patient with breast cancer demonstrating a mildly expansile, heterogeneously enhancing sternal lesion concerning for metastatic disease (circle). The patient also had suspected metastatic lesions involving several ribs. (C) Subsequent Tc-99m HDP SPECT CT, which confirmed metastatic disease in the sternum. Although there was suspicion for a pathologic sternal fracture, this diagnosis could not be made definitively on MRI.

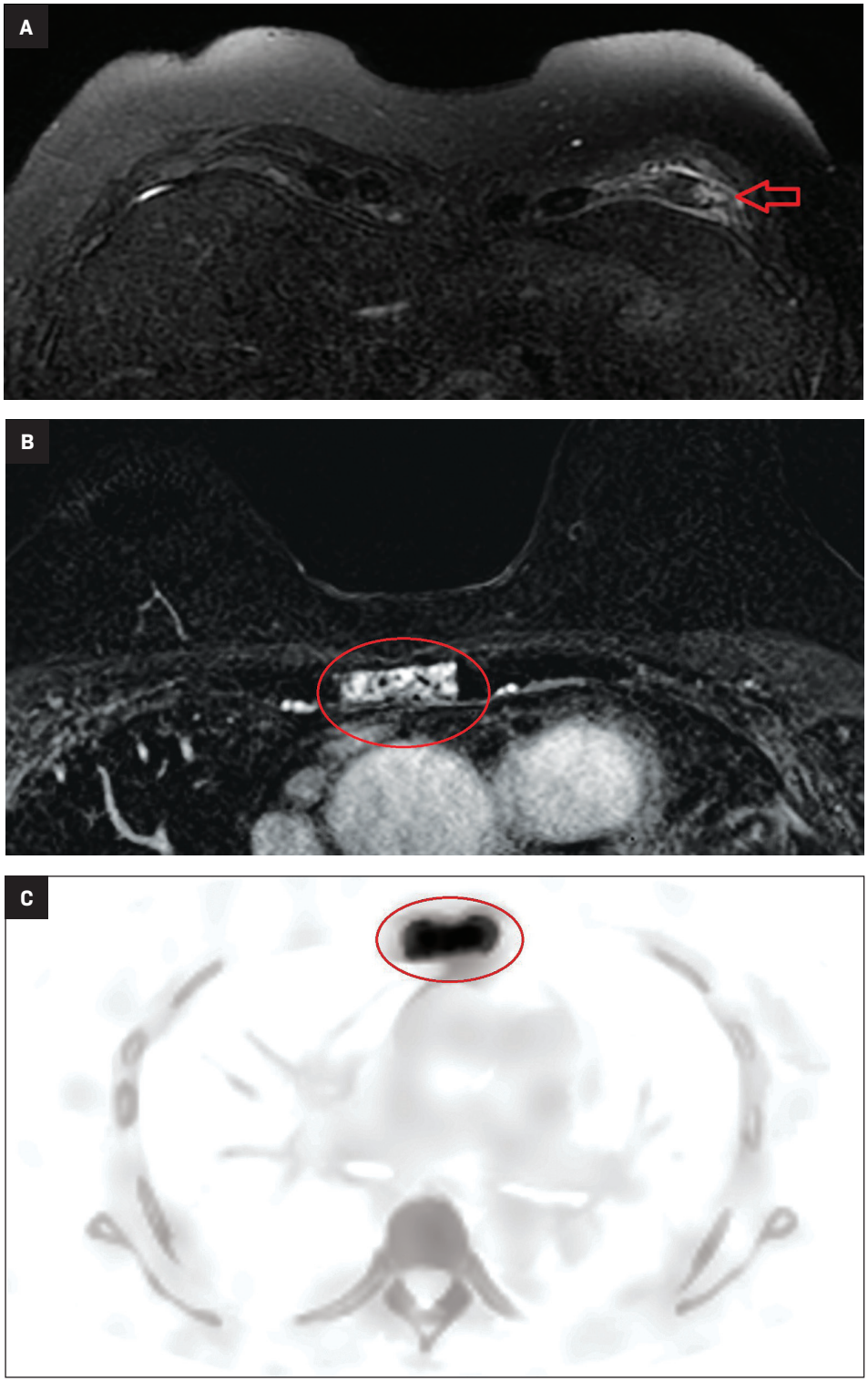

Figure 11. (A) T1 postcontrast subtracted image of the right breast in a patient with multiple myeloma showing an expansile, avidly enhancing, right anterior rib mass. Note the similar imaging features on MRI between multiple myeloma and other osseous metastases depicted in Figure 10. (B) Axial CT scan through the lesion shows the degree of associated osseous destruction (arrow).

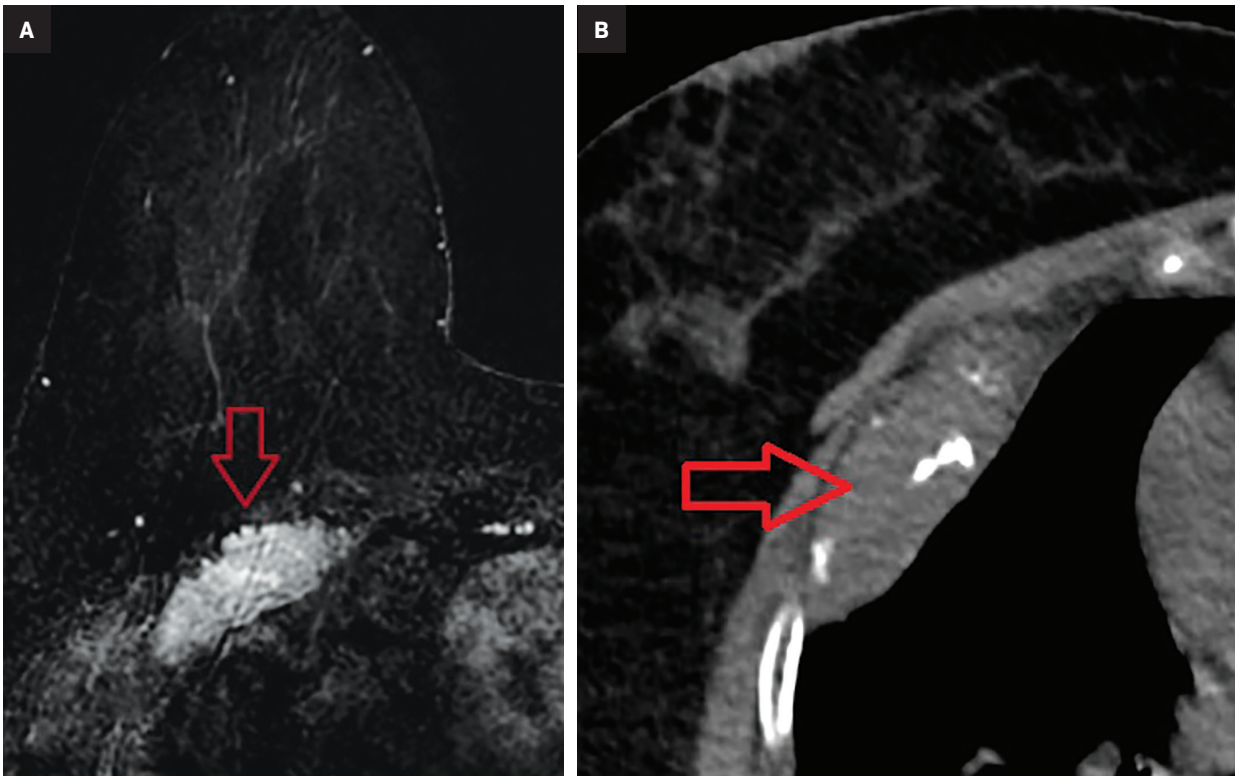

it is possible for a prominent disk to mimic a lesion to radiologists unfamiliar with its variations in appearance. Residual disks that have not ossified appear T2 hyperintense due to their cartilage content (Figure 9).

Rib and Sternal Fractures

Rib fractures are common in patients with chest wall trauma, occurring in about 10% of cases.[24] While chest CT has traditionally been the gold standard for assessing rib fractures, recent research has shown that MRI may be more sensitive for detecting acute fractures.[24] Additionally, elderly female patients and those who have received chest wall radiation are at increased risk of osteoporosis and rib fractures.[5,25,26] Although rib and sternal fractures are more likely to be detected on breast MRI given their locations, evaluating the localizer images is important, as they may show vertebral pathology, including fractures.[27]

Acute Traumatic Injuries

An acute fracture should demonstrate either a clear line extending through the cortex of the bone or the presence of cortical buckling (Figure 10). There is often a history of chest wall trauma. During the acute phase (up to four weeks), there is T2 hyperintense edema and enhancement in and around the fracture site resulting from posttraumatic inflammatory changes. Often, multiple adjacent ribs are fractured in a linear pattern. Over time, as the fracture enters the subacute phase of healing, edema and contrast enhancement decrease as surrounding bony callous forms. Once the bone is fully healed, enhancement and edema resolve and the osseous callus coalesces, typically resulting in a chronic fracture deformity.

Additionally, MRI may detect costal cartilage fractures not visible on CT or radiography. These occur at either the sternochondral or costochondral junction and most often affect the first and second ribs.[28] A T2 bright, linear fluid cleft extending through the costal cartilage with surrounding edema will be visible on MRI.

Pathologic Fractures

In contrast to their benign counterparts, pathologic fractures occur in the setting of malignancy such as metastatic disease (Figure 10) or multiple myeloma (Figure 11). The imaging features of both types of fractures can overlap; these include T2 hyperintense edema in and around the affected bone. Although diagnosing a pathologic fracture can be challenging with MRI alone, the presence of an expansile bone lesion or soft-tissue component may suggest a pathologic fracture. Discrete fracture lines may not be seen; bone lesions may slowly grow and erode through cortical bone, making it difficult to assess for an associated fracture.[29] Unless displacement is

Figure 12. (A) Large chondrosarcoma on a T1 fat-suppressed postcontrast image (star). Mineralization within the tumor is not readily apparent on MRI, but (B) axial noncontrast CT demonstrates the "ring and arc" pattern typical of chondroid lesions (red arrow). Expansion and extensive periosteal reaction of a left lateral rib denote the suspected origin site (white arrow). (C) A T1 fat-suppressed MR image demonstrates a large, irregular mass arising from a left-side rib with low-signal mineralization. (D) Axial CT shows extensive internal mineralization as areas of high density. Osteosarcoma was confirmed histologically.

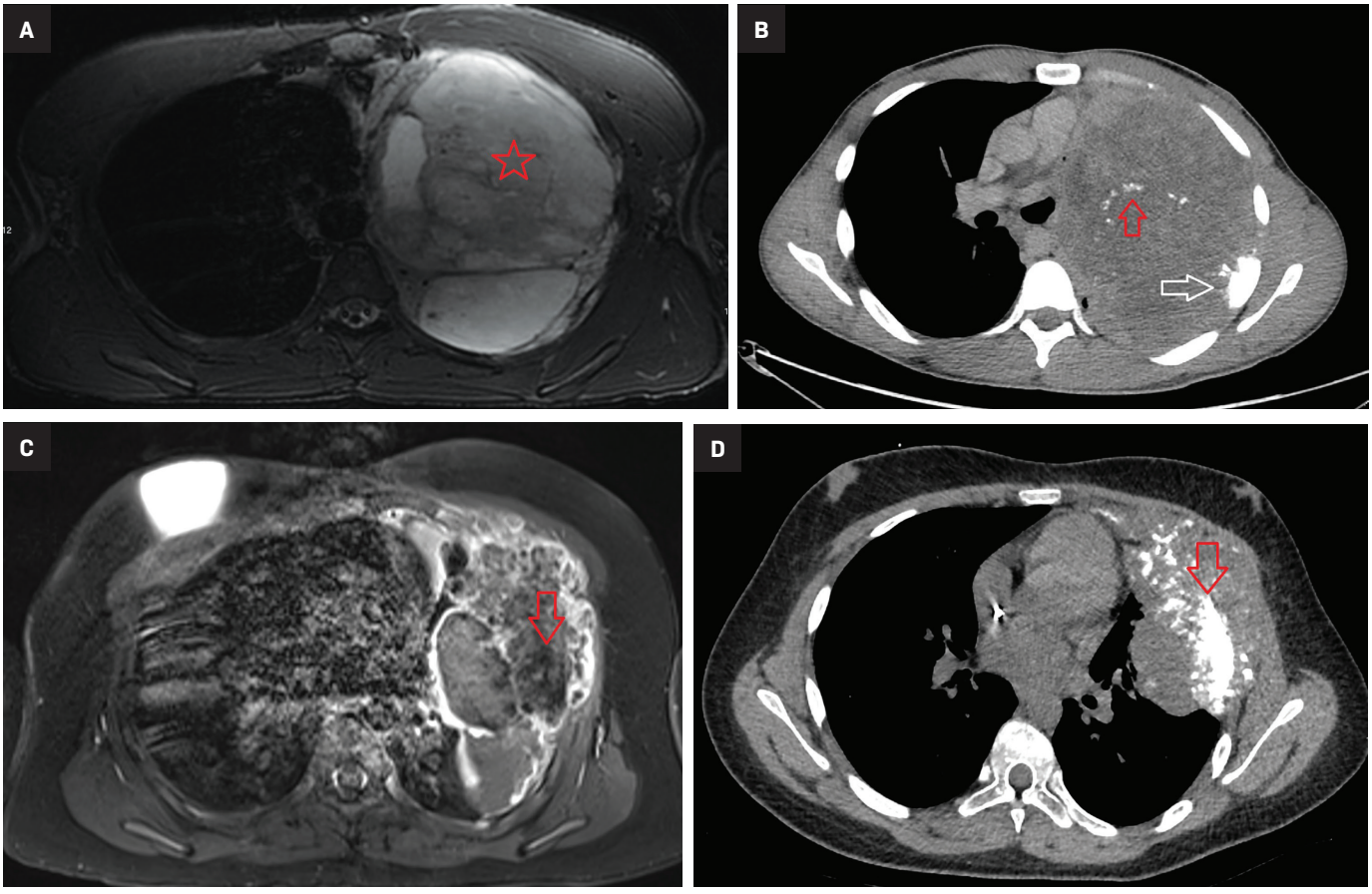

clearly visible, diagnosing a pathologic fracture on MRI may be difficult; CT may be helpful in equivocal cases. In contrast to the expected linear pattern of acute rib fractures, pathological fractures will generally follow a random distribution.

Chest Wall Malignancy

Metastatic Disease

The skeletal system is the most common site of distant breast cancer metastases (occurring in approximately 60% of patients with metastatic disease).[5] Other tumors that commonly spread to the bones include non-small cell lung cancer, hepatocellular carcinoma, renal cell carcinoma, thyroid cancer, and prostate cancer.[30] Discovery of osseous metastases on MRI immediately upstages a patient and usually alters the goal of therapy from cure to long-term remission. However, curative treatment may still be pursued if only a few metastases (oligometastases) are present.[31]

On MRI, metastatic lesions are typically T1 hypointense, owing to the replacement of normal fatty marrow by tumor cells, with associated T2 hyperintense marrow edema and avid contrast enhancement. While early osseous metastases are typically confined to bone, over time they may grow and invade through the cortex into adjacent soft tissues, increasing the risk for pathologic fracture. Metastases may become sclerotic following treatment, subjectively signifying interval healing. These changes, which are more apparent on CT, may be difficult to appreciate on MRI alone.

Multiple Myeloma

Multiple myeloma is the second-most common malignancy involving the skeleton (after metastatic disease) and is also the second-most common hematological malignancy (after non-Hodgkin lymphoma),[32] typically occurring in patients older than 50. Imaging features overlap with metastatic disease: T1 hypointense masses with intermediate or high T2 signal with avid enhancement (Figure 10). Computed tomography and radiography will demonstrate the classic "punched-out" appearance of numerous lytic lesions throughout the bones.

Multiple myeloma may also present extraskeletally as an extramedullary plasmacytoma. This lesion appears as a homogeneously enhancing mass, with variable and nonspecific T1 and T2 signal characteristics. The presence of myeloma elsewhere in the body may suggest a diagnosis of extramedullary plasmacytoma. The skin, muscles, and pleura are the most common sites of involvement.[33]

Primary Malignant Chest Wall Tumors

Multiple types of primary bone and soft-tissue tumors can occur in the chest wall, many of which share imaging features. However, some imaging features can suggest a diagnosis based on their location and appearance, with tissue sampling generally required for definitive diagnosis. Chondrosarcoma, osteosarcoma, and the Ewing sarcoma family of tumors often arise from the ribs and sternum. Soft-tissue tumors of the chest wall include angiosarcoma, liposarcoma, rhabdomyosarcoma, and lymphoma.

Malignant Tumors Arising from Ribs and Sternum

Chondrosarcoma (Figure 12) is the most common primary chest wall tumor in adults. It typically arises from the costal cartilage or the costochondral junction but may also result from malignant degeneration of an osteochondroma or enchondroma, especially in patients who have received chest wall radiation.[34] On MRI chondrosarcoma has low or intermediate T1 signal, high T2 signal, and avid enhancement. Areas of low T1 and T2 signal correspond with mineralization in the tumor, which on CT or radiographs corresponds to the typical "ring and arc" appearence of these tumors.

Osteosarcoma (Figure 12) is the most common primary bone tumor in adults. It commonly involves the long bones, but involvement of the ribs and sternum is also possible.[35] It typically arises within the marrow space of the bones, but certain subtypes can arise from the cortex (parosteal and periosteal subtypes) and soft tissues (extraskeletal osteosarcoma). While most osteosarcomas arise de novo, secondary subtypes can result from malignant degeneration of lesions such as fibrous dysplasia or Paget's disease, or radiation exposure.[35] MRI features include intermediate T1 signal, moderate-to-high T2 signal, heterogeneous enhancement, and areas of hemorrhage in the tumor. Typically, there is a high degree of mineralization within the tumor which will be T1 and T2 hypointense and be better visualized by CT or radiography.

The Ewing sarcoma family of tumors usually occurs in children and young adults and often presents as a painful, palpable, rapidly growing mass. In the chest, the ribs and scapulae are commonly involved sites.[36] On MRI, Ewing sarcoma typically has intermediate T1 signal, low or intermediate T2 signal, heterogeneous enhancement, and no internal mineralization. Rarely, the Ewing sarcoma family of tumors can arise directly from the soft tissues.[36]

Malignant Tumors Arising from Soft Tissues

The differential diagnosis of primary soft-tissue chest wall tumors is broad, with overlapping imaging features among many. A few do have a characteristic appearance on MRI. Liposarcomas are fat-containing masses with areas of enhancement or soft-tissue nodularity. Angiosarcomas demonstrate T1 intermediate signal, T2 hyperintensity, diffuse enhancement, and skin involvement.[37] Secondary angiosarcomas commonly occur following breast conservation surgery. The most common risk factors for these are prior radiation therapy and chronic lymphedema.[37] They may occur inside the breast or elsewhere in the chest wall. Angiosarcomas can be associated with a wide array of genetic syndromes, including type-1 neurofibromatosis, Maffucci syndrome, *BRCA 1* and *BRCA* 2, and others.

Lymphoma of the chest wall demonstrates greater signal homogeneity and enhancement compared to other chest wall tumors.[38] Rhabdomyosarcomas occur primarily in children, rarely in young adults. They demonstrate nonspecific imaging features and are not commonly seen on breast MRI.

Conclusion

Incidental musculoskeletal findings are common on breast MRI; it is important for radiologists to be able to identify these lesions, suggest a differential diagnosis, and guide management. While benign lesions often present with classic imaging features, many malignant lesions involving the chest share overlapping imaging features and may require correlation with CT or radiography to assess mineralization, as well as biopsy for definitive diagnosis. Recognizing these extramammary musculoskeletal findings is important, especially in patients with breast cancer, as they can impact staging, treatment, and therapeutic goals.

By reviewing the demographics and imaging features of benign and malignant chest wall lesions, radiologists can produce more specific reports, accelerate treatment planning, and help alleviate patient uncertainty and anxiety.

For further reading, we recommend the Society of Skeletal Radiology's white paper, *Guidelines for the Diagnostic Management of Incidental Solitary Bone Lesions on CT and MRI in Adults: Bone Reporting and Data System (Bone-RADS)*. This document offers a step-by-step flowchart based on their signal characteristics and other features.[39]

References

1) Iodice D, Di Donato O, Liccardo I, et al. Prevalence of extramammary findings on breast MRI: a large retrospective single-centre study. *Radiol Med*. 2013;118(7):1109-1118. doi:10.1007/s11547-013-0937-8

2) Moschetta M, Telegrafo M, Rella L, Stabile Ianora AA, Angelelli G. Let's go out of the breast: prevalence of extra-mammary findings and their characterization on breast MRI. *Eur J Radiol*. 2014;83(6):930-934. doi:10.1016/j.ejrad.2014.02.022

3) Rinaldi P, Costantini M, Belli P, et al. Extra-mammary findings in breast MRI. *Eur Radiol*. 2011;21(11):2268-2276. doi:10.1007/s00330-011-2183-6

4) Padia SA, Freyvogel M, Dietz J, Valente S, O'Rourke C, Grobmyer SR. False-positive extra-mammary findings in breast MRI: Another cause for concern. *Breast J*. 2016;22(1):90-95. doi:10.1111/tbj.12524

5) Gao Y, Ibidapo O, Toth HK, Moy L. Delineating extramammary findings at breast MR imaging. *Radiographics*. 2017;37(1):10-31. doi:10.1148/rg.2017160051

6) Ulano A, Bredella MA, Burke P, et al. Distinguishing untreated osteoblastic metastases from enostoses using CT attenuation measurements. *AJR Am J Roentgenol*. 2016;207(2):362-368. doi:10.2214/AJR.15.15559

7) Bedard T, Mohammed M, Serinelli S, Damron TA. Atypical enostoses-Series of ten cases and literature review. *Medicina (Kaunas)*. 2020;56(10):534. Published 2020 Oct 13. doi:10.3390/medicina56100534

8) Nielsen G, Baumhoer D, Bredella M, Sumathi V. *WHO classification of tumours: Soft tissue and bone tumours*. 5th ed, vol. 3. Lyon, France. International Agency for Research on Cancer; 2020.

9) Murphey MD, Fairbairn KJ, Parman LM, Baxter KG, Parsa MB, Smith WS. From the archives of the AFIP. Musculoskeletal angiomatous lesions: radiologic-pathologic correlation. *Radiographics*. 1995;15(4):893-917. doi:10.1148/radiographics.15.4.7569134

10) Kadu VV, Saindane KA, Goghate N, Goghate N. Osteochondroma of the rib: a rare radiological appearance. *J Orthop Case Rep*. 2015;5(1):62-64. doi:10.13107/jocr.2250-0685.258

11) Murphey MD, Choi JJ, Kransdorf MJ, Flemming DJ, Gannon FH. Imaging of osteochondroma: variants and complications with radiologic-pathologic correlation. *Radiographics*. 2000;20(5):1407-1434. doi:10.1148/radiographics.20.5.g00se171407

12) Fitzpatrick KA, Taljanovic MS, Speer DP, et al. Imaging findings of fibrous dysplasia with histopathologic and intraoperative correlation. *AJR Am J Roentgenol*. 2004;182(6):1389-1398. doi:10.2214/ajr.182.6.1821389

13) Traibi A, El Oueriachi F, El Hammoumi M, Al Bouzidi A, Kabiri el H. Monostotic fibrous dysplasia of the ribs. *Interact Cardiovasc Thorac Surg*. 2012;14(1):41-43. doi:10.1093/icvts/ivr048

14) Gaskin CM, Helms CA. Lipomas, lipoma variants, and well-differentiated liposarcomas (atypical lipomas): results of MRI evaluations of 126 consecutive fatty masses. *AJR Am J Roentgenol*. 2004;182(3):733-739. doi:10.2214/ajr.182.3.1820733

15) Tateishi U, Gladish GW, Kusumoto M, et al. Chest wall tumors: radiologic findings and pathologic correlation: Part 1. Benign tumors. *Radiographics*. 2003;23(6):1477-1490. doi:10.1148/rg.236015526

16) Suh JS, Abenoza P, Galloway HR, Everson LI, Griffiths HJ. Peripheral (extracranial) nerve tumors: correlation of MR imaging and histologic findings. *Radiology*. 1992;183(2):341-346. doi:10.1148/radiology.183.2.1561333

17) Burk DL Jr, Brunberg JA, Kanal E, Latchaw RE, Wolf GL. Spinal and paraspinal neurofibromatosis: surface coil MR imaging at 1.5 T1. *Radiology*. 1987;162(3):797-801. doi:10.1148/radiology.162.3.3101136

18) Raikos A, Paraskevas GK, Tzika M, et al. Sternalis muscle: an underestimated anterior chest wall anatomical variant. *J Cardiothorac Surg*. 2011;6:73. doi:10.1186/1749-8090-6-73

19) Georgiev GP, Jelev L, Ovtscharoff VA. On the clinical significance of the sternalis muscle. *Folia Med (Plovdiv)*. 2009;51(3):53-56.

20) Sebes JI, Salazar JE. The manubriosternal joint in rheumatoid disease. *AJR Am J Roentgenol*. 1983;140(1):117-121. doi:10.2214/ajr.140.1.117

21) Becker NJ, de Smet AA, Cathcart-Rake W, Stechschulte DJ. Psoriatic arthritis affecting the manubriosternal joint. *Arthritis Rheum*. 1986;29(8):1029-1031. doi:10.1002/art.1780290814

22) Sugimoto H, Tamura K, Fujii T. The SAPHO syndrome: defining the radiologic spectrum of diseases comprising the syndrome. *Eur Radiol*. 1998;8(5):800-806. doi:10.1007/s003300050475

23) Ehara S. Manubriosternal joint: imaging features of normal anatomy and arthritis. *Jpn J Radiol*. 2010;28(5):329-334. doi:10.1007/s11604-010-0438-9

24) Zhang T, Wu J, Chen YC, Wu X, Lu L, Mao C. Magnetic resonance imaging has better accuracy in detecting new-onset rib fractures as compared to computed tomography. *Med Sci Monit*. 2021;27:e928463. Published 2021 Jan 11. doi:10.12659/MSM.928463

25) Prins JTH, Van Lieshout EMM, Reijnders MRL, Verhofstad MHJ, Wijffels MME. Rib fractures after blunt thoracic trauma in patients with normal versus diminished bone mineral density: a retrospective cohort study. *Osteoporos Int*. 2020;31(2):225-231. doi:10.1007/s00198-019-05219-9

26) Way AR, Wasserman PL, Mailhot R, Letter H. Radiation-Induced Rib Fractures on Magnetic Resonance Imaging Following Proton Therapy for Breast Cancer With Pencil Beam Scanning. *Cureus*. 2020;12(10):e11120. doi:10.7759/cureus.11120

27) Bazzocchi A, Spinnato P, Garzillo G, et al. Detection of incidental vertebral fractures in breast imaging: the potential role of MR localisers. *Eur Radiol*. 2012;22(12):2617-2623. doi:10.1007/s00330-012-2521-3

28) Subhas N, Kline MJ, Moskal MJ, White LM, Recht MP. MRI evaluation of costal cartilage injuries. *AJR Am J Roentgenol*. 2008;191(1):129-132. doi:10.2214/AJR.07.3396

29) Marshall RA, Mandell JC, Weaver MJ, Ferrone M, Sodickson A, Khurana B. Imaging features and management of stress, atypical, and pathologic fractures. *Radiographics*. 2018;38(7):2173-2192. doi:10.1148/rg.2018180073

30) Shupp AB, Kolb AD, Mukhopadhyay D, Bussard KM. Cancer metastases to bone: Concepts, mechanisms, and interactions with bone osteoblasts. *Cancers (Basel)*. 2018;10(6):182. Published 2018 Jun 4. doi:10.3390/cancers10060182

31) Terao M, Niikura N. Diagnosis of oligometastasis. *Transl Cancer Res*. 2020;9(8):5032-5037. doi:10.21037/tcr.2020.01.04

32) Ormond Filho AG, Carneiro BC, Pastore D, et al. Whole-body imaging of multiple myeloma: Diagnostic criteria. *Radiographics*. 2019;39(4):1077-1097. doi:10.1148/rg.2019180096

33) Bladé J, Beksac M, Caers J, et al. Extramedullary disease in multiple myeloma: a systematic literature review. *Blood Cancer J*. 2022;12(3):45. doi:10.1038/s41408-022-00643-3

34) Singh A, Chandrashekhara SH, Triveni GS, Kumar P. Imaging in sternal tumours: A pictorial review. *Pol J Radiol*. 2017;82:448-456. doi:10.12659/PJR.901226

35) Murphey MD, Robbin MR, McRae GA, Flemming DJ, Temple HT, Kransdorf MJ. The many faces of osteosarcoma. *Radiographics*. 1997;17(5):1205-1231. doi:10.1148/radiographics.17.5.9308111

36) Murphey MD, Senchak LT, Mambalam PK, Logie CI, Klassen-Fischer MK, Kransdorf MJ. From the radiologic pathology archives: Ewing sarcoma family of tumors: radiologic-pathologic correlation. *Radiographics*. 2013;33(3):803-831. doi:10.1148/rg.333135005

37) Gaballah AH, Jensen CT, Palmquist S, et al. Angiosarcoma: clinical and imaging features from head to toe. *Br J Radiol*. 2017;90(1075):20170039. doi:10.1259/bjr.20170039

38) Witte B, Hürtgen M. Lymphomas presenting as chest wall tumors. *Thorac Surg Sci*. 2006;3:Doc01.

39) Chang CY, Garner HW, Ahlawat S, et al. Society of Skeletal Radiology- white paper. Guidelines for the diagnostic management of incidental solitary bone lesions on CT and MRI in adults: Bone reporting and data system (Bone-RADS). *Skeletal Radiol*. 2022;51(9):1743-1764. doi:10.1007/s00256-022-04022-8